Turkish Journal of Earth Sciences

Volume 33
Number 1 *SI-1*

Article 6

1-4-2024

Response of water resources to the Kahramanmaraş earthquakes (MW 7.7 and MW 7.6) that occurred on February 6, 2023, on the East Anatolian Fault Zone (Türkiye)

CELALETTİN ŞİMŞEK
celalettin@deu.edu.tr

GÖRKEM AKINCI
gorkem.akinci@deu.edu.tr

OKAN FISTIKOĞLU
okan.fistikoglu@deu.edu.tr

KEREM CANLI
kerem.canli@deu.edu.tr

HASAN SÖZBİLİR
hasan.sozbilir@deu.edu.tr

See next page for additional authors

Recommended Citation

ŞİMŞEK, CELALETTİN; AKINCI, GÖRKEM; FISTIKOĞLU, OKAN; CANLI, KEREM; SÖZBİLİR, HASAN; AYOL, AZİZE; and BİLGİÇ, EFEM (2024) "Response of water resources to the Kahramanmaraş earthquakes (MW 7.7 and MW 7.6) that occurred on February 6, 2023, on the East Anatolian Fault Zone (Türkiye)," *Turkish Journal of Earth Sciences*: Vol. 33: No. 1, Article 6. https://doi.org/10.55730/1300-0985.1899
Available at: https://journals.tubitak.gov.tr/earth/vol33/iss1/6

Turkish Journal of Earth Sciences

http://journals.tubitak.gov.tr/earth/

Research Article

Turkish J Earth Sci
(2024) 33: 69-84
© TÜBİTAK
doi:10.55730/1300-0985.1899

Response of water resources to the Kahramanmaraş earthquakes (MW 7.7 and MW 7.6) that occurred on February 6, 2023, on the East Anatolian Fault Zone (Türkiye)

Celalettin ŞİMŞEK[1,*], **Görkem AKINCI**[2], **Okan FISTIKOĞLU**[3], **Kerem CANLI**[4], **Hasan SÖZBİLİR**[5], **Azize AYOL**[6], **Efem BİLGİÇ**[6]

[1]Torbalı Technical Vocational School of Higher Education, Dokuz Eylül University, İzmir, Turkiye
[2]Science and Technology Application and Research Center, Dokuz Eylül University, İzmir, Turkiye
[3]Water Resources Management, Water-Natural Disasters Research and Application Center, Dokuz Eylül University, İzmir, Turkiye
[4]Department of Biology, Faculty of Science, Dokuz Eylül University, İzmir, Turkiye
[5]Earthquake Research and Application Center, Dokuz Eylül University, İzmir, Turkiye
[6]Department of Environmental Engineering, Faculty of Engineering, Dokuz Eylül University, İzmir, Turkiye

Received: 24.04.2023 • **Accepted/Published Online:** 21.06.2023 • **Final Version:** 04.01.2024

Abstract: On February 6, 2023, two destructive earthquakes of 7.7 M_W and 7.6 M_W occurred in Pazarcık (Kahramanmaraş) and Elbistan (Kahramanmaraş) at 04:17 and 13:24 hours, respectively. These earthquakes caused a surface rupture with a total length of 450 km in the region with an average displacement of 3 m between the Arabian and Anatolian plates. This study was conducted to investigate the physical deformation of the aquifer system and the current water quality characteristics in the affected region utilizing field observations and on-site analysis of water sources and tap water. The study revealed significant physical changes in the karstic springs and groundwater wells, including turbidity discharges from all karstic springs due to the limestone-covered terra rosa soils in the region, destruction of groundwater wells near the coastal alluvial aquifer due to liquification, significant intrusion of sea water due to settlements caused by liquefaction in the alluvial aquifer, presence of microbiological pathogens carried by particles creating turbidity in the water sources, and presence of microbiological pathogens in some tap waters due to contamination by pollutants resulting from damage to the water and sewerage networks. These preliminary findings suggest that the earthquake-induced shaking and physical deformation impacted the quality of groundwater sources and tap water in the region.

Key words: Aquifer deformation, groundwater, microbiology, tap water, turbidity, postearthquake effects

1. Introduction

Earthquake shock waves and the resulting fractures can have a significant impact not only on surface structures but also on groundwater resources. Numerous studies have investigated the postearthquake changes in groundwater sources, which are considered reliable sources of water worldwide. These studies have generally focused on monitoring short- and long-term changes in groundwaters after earthquakes (Sato et al., 2000; Chia et al., 2008; Singh, 2008; Amoruso et al., 2011; Cox et al., 2012; Lee and Woo, 2012; Cheong et al., 2013; Wang and Manga, 2015; Nakagawa et al., 2019). The changes observed include alterations in groundwater levels, changes in the flow regimes of springs or streams, and shifts in the temperatures of some geothermal wells, where physiochemical changes may be linked to the contamination from soil liquefaction. Among these changes, the most significant have been detected in groundwater levels, which have ranged between 1.0 cm to 10.0 m in postearthquake periods (Chia et al., 2008; Cheong et al., 2013).

Studies have also revealed that hydrogeologic responses to earthquakes can include changes in flow rates in spring systems and alterations to river flow regimes (Mohr et al., 2015). Sato et al. (2000) found that the flow velocities in several springs had increased due to secondary permeability development following the 1995 Kobe earthquake. In a detailed study conducted after the 2016 Kumamoto earthquake in Japan, it was discovered that most shallow wells exhibited limited changes in groundwater level during the earthquake shock, but significant differences were observed in the postearthquake period. Previous research has also revealed that after the rise or drop the groundwater level typically returns to its previous state within a short to medium period after an earthquake (Hosono et al., 2019; Nakagawa et al., 2019, 2020).

* Correspondence: celalettin@deu.edu.tr

Changes in the physiochemical and microbiological quality of water resources in postearthquake periods have also been monitored (Skelton et al., 2014). One of the most common physicochemical changes observed in water resources after an earthquake is increased turbidity. Turbidity is caused by large numbers of suspended organic and inorganic particles including sediments and microscopic organisms that are carried by the moving water through rocks and soil and into the groundwater (WHO, 2008). The movement of loose sediments from rock pores, cracks, and cover layers during earthquakes can cause groundwater to become turbid. This turbidity is often seen in springs and wells and is typically temporary, with the water returning to its original state in a short period of time. However, it has been found that the number of microbiological pathogens in karstic springs increases with turbidity (WHO, 2008). In addition, liquefaction can lead to an increase in microbiological pathogens in water due to changes in the filtration properties of the ground caused by earthquakes (Karmakar et al., 2008; Ito et al., 2020).

According to Favere et al. (2021), contamination of drinking water sources with sewage and overflow into waterways is possible during heavy rainfall, especially in areas with old water infrastructure. Following an earthquake, fractures in infrastructure systems can lead to microbial contamination and pose a significant threat to the safety and quality of water sources in affected regions, often leading to an increased risk of waterborne diseases and affecting vulnerable populations, particularly children (Karmakar et al., 2008; Ito et al., 2020).

Previous studies have highlighted the changes in water sources and the prevalence of waterborne infections after earthquakes. For instance, after the Gorkha earthquake, households experienced changes in the quality of supplied water, forcing them to drink bottled water or resort to relatively cheaper tanker water or freely available groundwater (Ito et al., 2020). The earthquake in Kashmir in 2005 led to widespread contamination of drinking water sources, resulting in a common-source outbreak of rotavirus gastroenteritis among infants and small children (Karmakar et al., 2008). In disaster-affected areas, waterborne infections have sometimes been responsible for more fatalities than the disaster itself (Maleki et al., 2020).

Several pathogens have been identified in water sources after the earthquakes. These include *Escherichia coli*, *Helicobacter pylori*, *Staphylococcus aureus*, and other waterborne pathogens such as *Legionella* spp., *Enterococci* spp., *Aeromonas* spp., *Bacillus* spp., *Burkholderia pseudomallei*, *Klebsiella* spp., *Campylobacter* spp., and *Yersinia* spp. (Maleki et al., 2020).

After the 2010 earthquake in Haiti, the introduction of cholera resulted in many thousands of cases and deaths, emphasizing the ongoing threat of waterborne diseases in disaster situations. Similarly, waterborne diseases remain a significant burden in low-income countries, particularly after natural disasters or warfare, as seen in Yemen in 2017 (Tulchinsky, 2018; Maleki et al., 2020).

Catastrophic earthquakes can cause severe damage not only to the water distribution networks but also the water treatment plants. Due to damage to the whole water distribution system, from the reservoir to the tap water, significant water interruptions may occur (Kuraoka and Rainer, 1996). Water treatment systems are among the few public facilities that have a direct impact on the population in an earthquake zone (Schiff, 1995; Zare et al., 2010). In the İzmit (Türkiye) earthquake of August 17, 1999, which was one of the most devastating earthquakes in the country, significant damage occurred in all water-conveying systems and treatment plants (Scawthorn and Johnson, 2000).

Many past studies have been conducted to determine the effects of earthquakes on the quality of water resources. However, obtaining the first observations on the quality of water resources after devastating earthquakes in Türkiye is of high importance, since the quality of potable water directly affects the health of people who have survived in the region. In this study, it is aimed to reveal the short-term effects of the Kahramanmaraş earthquakes on the physical and microbiological properties of groundwater, where most of the drinking water is sourced from groundwater in the region. The findings are also vital for the planning of postearthquake water management strategies.

2. Characteristics of the study area

The study area covers the East Anatolian Fault Zone (EAFZ) and its surroundings, as shown in Figure 1. The geomorphological structure of the earthquake region mainly consists of the Taurus belt and the surrounding plains. The study area rises from south to north and, due to its elevation, experiences a transition from a Mediterranean climate to a continental climate. This situation is shaped by the Taurus mountain belt extending towards the north and other parallel mountain belts. Plains of different heights have formed between these mountain belts and various human activities within agricultural, residential, and industrial areas take place on these plains. The Malatya, Kahramanmaraş, Gaziantep, Osmaniye, Adana, and Hatay provinces are located in the region from north to south, respectively. The study area has a total population of 13 million according to 2023 data (TÜİK, 2023). The study area location map showing the corresponding provinces is presented in Figure 1.

2.1. Geology and hydrogeological setting

The EAFZ is one of the most important seismic sources in terms of earthquake risk in Türkiye. It occurred during

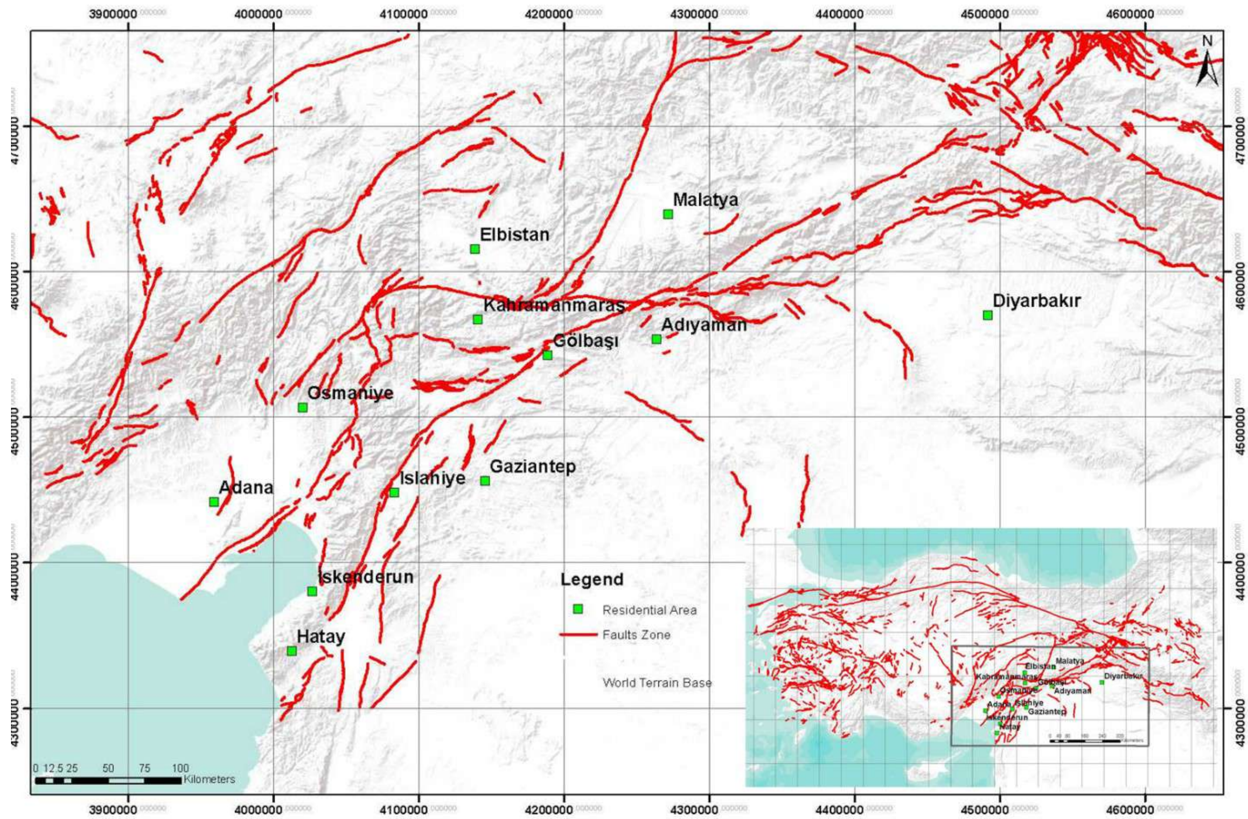

Figure 1. Location of the study area. (Modified from Duman and Emre, 2013;Karabacak et.al., 2023)

the neotectonic regime in Eastern Anatolia with an intracontinental left-lateral strike-slip fault zone that forms the border between the Arabian Plate and the Anatolian Block (Şengör et al., 1985). The NE-SW trending EAFZ, which merges with the North Anatolian Fault Zone (NAFZ) at the Karlıova (Bingöl) triple junction in the northeast and the Dead Sea Fault Zone (ÖDFZ) in the Amik Basin in the southwest, has a length of approximately 600 km (Saroglu et al., 1992). The EAFZ has been divided into different numbers of segments by researchers based on its geometry (Duman and Emre, 2013).

In previous studies, the presence of the EAFZ, which was first mapped as a lineament between Karlıova and Bingöl by Altınlı (1963) and Ketin (1966), was first described by Allen (1969). The zone was the subject of study by many researchers (Arpat and Şaroğlu, 1972; Ambraseys, 1989) after the 1971 Bingöl earthquake (M: 6.8), and it was named the "East Anatolian Fault Zone" and mapped up to the Amik Basin by Arpat and Şaroğlu (1972). Considering the studies carried out in recent years, Duman and Emre (2013) analyzed the EAFZ by dividing it into two branches, north and south. These researchers accepted the southern branch, which they stated to have a length of approximately 600 km between Karlıova (Bingöl) and Antakya, as the main branch and suggested that it merged with the ÖDFZ and the Cyprus Arc at the Amik (Hatay) triple junction.

Historical earthquake records indicate that the EAFZ has the potential to produce significant earthquakes. The most recent of these earthquakes occurred on February 6, 2023. Based on detailed research related to the general characteristics of the EAFZ, when the Pazarcık (Kahramanmaraş, Türkiye) earthquake (M_W = 7.7) and Elbistan (Kahramanmaraş, Türkiye) earthquake (M_W = 7.6) occurred, neighboring active fault systems were fractured in succession between the Hatay and Malatya zones. As a result of the earthquakes, a fracture zone with a total length of 450 km was caused to rupture and an average displacement of 3 m occurred between the Arabian and Anatolian plates. Although there was an average displacement of 3 m, lateral shifts of up to 7.0 m occurred in some parts (Karabacak et al., 2023), and the displacement and earthquake shocks caused the collapse of thousands of buildings and the deaths of more than 50,000 people. The devastating earthquakes caused many unusual geological disasters and deformations in the rocks, such as liquefaction, settlement, fracture lines, displacement, and local landslides.

The study area and its surroundings, in terms of stratigraphy, structural features, and rock type, have several tectonostratigraphic units tectonically related to each other (Figure 2). The rocks are in the Precambrian-Eocene age range from the basement. These units are mainly Paleozoic metamorphites, Mesozoic ophiolites and flysch, Paleogene sedimentary rocks, Neogene volcano-sedimentary rocks, and Quaternary sediments, (Aksoy, 1994; Tatar et al., 1995; Beyarslan and Bingöl, 2018). Of these units, the Precambrian and Paleozoic metamorphic rocks are the basement rock, on which Mesozoic-aged flysch and ophiolitic series lies with unconformity via a thrust fault. In general, metamorphic basement rocks are observed mainly as schists and marble to a wide extent along the EAFZ zone of the study area. The Mesozoic flysch consists of mainly mudstone and metasandstone including allochthonous limestones as shown in Figure 2. A wide portion of the study area is mostly characterized by Paleogene and Neogene series including conglomerates, sandstones, claystones, clayey limestones, and marl. Finally, most of the plains of the study area are primarily covered by alluvial layers.

A detailed assessment of the regional geology reveals that the most important water-bearing units in the study area are karstic aquifers such as marble, allochthonous limestone, and clayey limestone. The high-discharge springs originating from these karstic units have discharge rates from 300 to 4000 L/s. The Neogene series (conglomerate-sandstone and clayey-limestone) aquifers and Quaternary alluvial aquifer systems are of secondary importance for the region as they have a relatively lower water supply potential compared to the karstic limestone units. Alluvial aquifers cover the plains in the Hatay, İskenderun, Adana, Elbistan, and Malatya areas of the region and provide a significant amount of groundwater through wells. In the earthquake zone, settlements areas have largely developed in locations with alluvial aquifers.

3. Materials and methods

A detailed study was begun after the catastrophic earthquakes in February 2023. The field work was conducted as a series of expeditions along the EAFZ. During this study, many damaged areas such as those of Hatay, Adana, Osmaniye, Gaziantep, Elbistan,

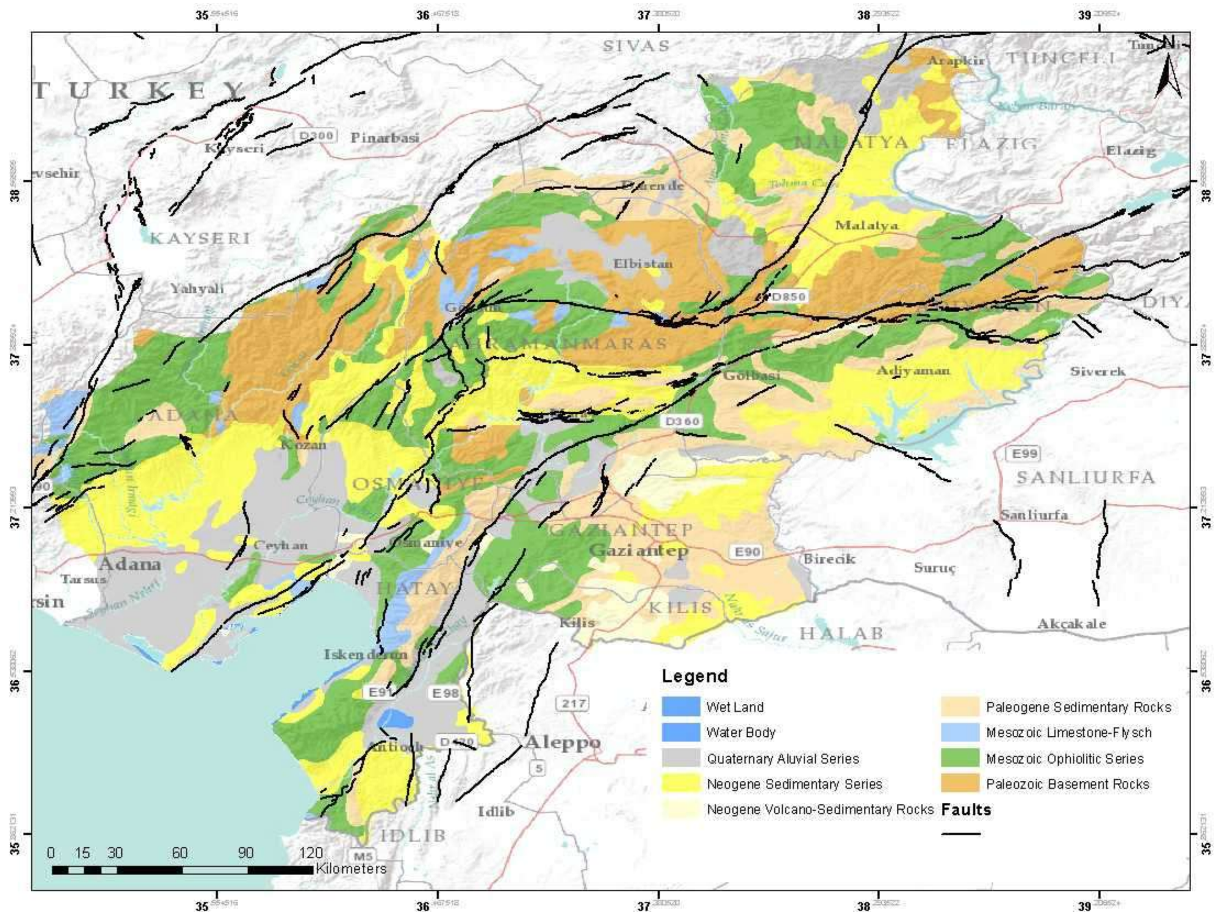

Figure 2. Geological map of the study area.

Kahramanmaraş, and Malatya were investigated and potential sampling locations within the study area (e.g., karstic springs and accessible wells) were also determined. In addition to potential drinking water resources in the field, samples were taken from drinking water treatment plants and drinking water network systems, such as tap water. In addition, sea intrusion waters were collected using clean buckets of 5 L rinsed with sampled water twice, while other samples were obtained into sample bottles directly from running or flowing water or from the outlets of operating pumps of wells. Details on the sampling points are given in Table 1. In total, 47 water points from which samples could be taken were selected for the field study. For physicochemical measurements and microbiological analyses of the water samples in the field studies, samples of (i) surface water, (ii) groundwater used for drinking water purposes, (iii) water from drinking and sewage treatment plants, and (iv) tap water were taken. The locations of the selected monitoring stations are presented in Figure 3.

The physicochemical properties of the water samples (temperature, pH, electrical conductivity, salinity, dissolved oxygen concentration, and saturation) were determined with a WTW Multi 360 IDS SET G device (Xylem Analytics, Weilheim, Germany) during the sampling. A sterilized cotton swab was wetted with running water (for samples from taps, surface waters, springs, groundwater wells, and water treatment plant inlets and outlets) or dipped into the sample bottle (for sea intrusion samples) and about 1 mL of sample was cultivated on sterilized agar medium in a petri dish under the flame of a battery-operated Bunsen burner onsite. Petri dishes were covered with glass lids and stored in sterile ice boxes at ambient temperature. The samples were transferred to a 25 °C incubator immediately after arrival to the laboratory; the minimum incubation time of the cultivated dishes was 5 days. After that, different colonies were collected with the help of a sterile swab, cultivated on agar, and left to incubate to be examined separately. The Gram staining method

Table 1. Sampling location properties.

Y	X	Sampling date	Location and properties	Province	Town
Water treatment plant (WTP)					
36.163881	36.029211	20.03.2023	Karaçay FWTP-Inlet	Hatay	Samandağ
36.163881	36.029211	20.03.2023	Karaçay FWTP-Outlet	Hatay	Samandağ
37.189800	35.263099	21.03.2023	Çatalan FWTP-Inlet	Adana	Karaisalı
37.189800	35.263099	21.03.2023	Çatalan FWTP-Outlet	Adana	Karaisalı
37.581137	37.027950	22.03.2023	Kahramanmaraş Ayvalı FWTP-Inlet	Kahramanmaraş	Dereköy
37.581137	37.027950	22.03.2023	Kahramanmaraş Ayvalı FWTP-Outlet	Kahramanmaraş	Dereköy
Spring water					
37.212282	36.567886	3.03.2023	Surfaced spring water used in irrigation-city center	Osmaniye	Bahçe
37.263217	36.624553	3.03.2023	Surfaced spring water-mountainous area	Osmaniye	Bahçe
36.129636	36.144137	20.03.2023	Harbiye waterfall-surfaced spring water	Hatay	Antakya
36.115043	36.124420	21.03.2023	Karst spring	Hatay	Defne/Döver
38.232519	38.282754	24.03.2023	Horata 1-surfaced spring water in concrete channel	Malatya	Kozluk, Yeşilyurt
38.232519	38.282754	24.03.2023	Horata 2-surfaced spring water in river bed	Malatya	Kozluk, Yeşilyurt
38.239947	38.274605	24.03.2023	Gündüzbey Kaptaj	Malatya	Yeşilyurt
Groundwater well (GWW)					
37.194197	36.722849	28.02.2023	GWW, next to Turgut Özal Viaduct	Gaziantep	Başpınar, Nurdağı
37.290551	37.579324	1.03.2023	Karst GWW-operated by municipality	Gaziantep	Karapınar, Yavuzeli
37.473748	37.637964	1.03.2023	GWW-operated by municipality	Gaziantep	Yolveren
37.416476	37.706250	1.03.2023	Wastewater treatment plant GWW (unused)	Gaziantep	Araban
36.995860	37.787830	1.03.2023	Cooking oil industry GWW	Gaziantep	Nizip
36.301399	36.199790	20.03.2023	GWW in oil station	Hatay	Antakya
36.258553	36.180249	20.03.2023	GWW in city center	Hatay	Antakya
36.58827	36.147683	20.03.2023	GWW in biological WWTP	Hatay	İskenderun

Table 1. (Continued).

36.830895	35.580752	21.03.2023	District GWW	Adana	Çatalpınar, Yüreğir
36.860629	35.543329	21.03.2023	GWW of a farm	Adana	Herekli, Yüreğir
37.027005	36.625283	22.03.2023	GWW at water network start point	Gaziantep	İslahiye
37.026835	36.644953	22.03.2023	GWW in central bus station	Gaziantep	İslahiye
37.546413	36.914090	22.03.2023	Municipality construction site GWW	Kahramanmaraş	Onikişubat
38.336536	37.055401	23.03.2023	Coal mining site-GWW in gyttja	Kahramanmaraş	Afşin-Elbistan
38.333723	37.116585	23.03.2023	Coal mining site-GWW in karst	Kahramanmaraş	Afşin-Elbistan
Surface water					
36.998180	37.785250	1.03.2023	Nizip Creek	Gaziantep	Nizip
37.376606	35.469705	21.03.2023	Sanko Sanibey Dam tail water	Adana	Aladağ
Tap water					
36.147496	36.054026	20.03.2023	Karaçay city center	Hatay	Karaçay, Samandağ
36.961491	35.350645	21.03.2023	Yüreğir biological WWTP	Adana	Yüreğir
37.183828	36.754840	22.03.2023	Small industrial site	Gaziantep	Nurdağı
37.572810	36.974300	22.03.2023	City center	Kahramanmaraş	Dulkadiroğlu
37.072559	37.376575	23.03.2023	City center	Gaziantep	Merkez
37.497348	37.311949	23.03.2023	City center	Kahramanmaraş	Pazarcık
38.340325	38.435892	24.03.2023	Teknokent-container city	Malatya	Battalgazi
Intrusion water					
36.589386	36.177384	20.03.2023	Intrusion water from bottom floor of a building	Hatay	İskenderun
36.589720	36.177104	20.03.2023	Intrusion water from earth surface	Hatay	İskenderun

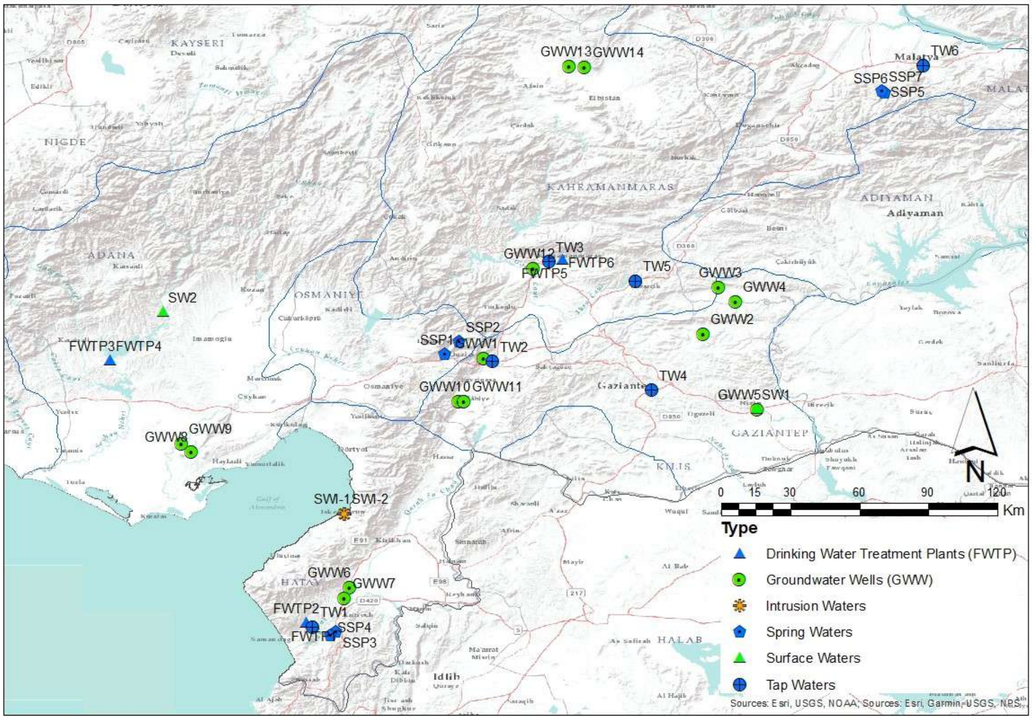

Figure 3. Distribution of water sampling points in the earthquake region.

was applied to observe gram-positive and gram-negative microorganisms. For gram-positive microorganisms, preparations were coated by adding crystal violet dye solution and left for 1 min, washed with sufficient distilled water, covered with the addition of Lugol solution, and left for 1 more min (Figures 4a and 4b).

For gram-negative microorganisms, preparations were washed with distilled water, 95% ethanol was added, and the preparations were left standing for 15 s. An aqueous fuchsin dye solution was then added, and after waiting 30 s, they were washed with sufficient distilled water (Figures 4c and d). Dried preparations were examined under a microscope and aerobic colony counts were measured in square centimeters for the samples.

4. Results

4.1. Changes in the sources of water

There are several karst springs with high discharge flow rates in the earthquake zone. These karst springs include the Hatay (Harbiye), Osmaniye (Bahçe), Gaziantep (Akpınar, Kırkgöz, and Karpuzatan), and Malatya (Derme) springs. These springs are used for drinking purposes in the region. After the earthquakes in the region, a significant turbidity problem occurred in these karstic springs. Field observations in the study area revealed that the lithological characteristics of the aquifer played an important role in the turbidity of the springs. In particular, partial turbidity was observed in springs originating from allochthonous limestones, while high turbidity was observed in springs originating from a clayey limestone karstic system. In this context, high-flow spring systems discharging from the karstic system in the earthquake zone are discussed in detail below.

One of most important springs in the eastern part of Türkiye is the Derme karst spring. The Derme spring discharges from Paleo-Carboniferous limestone and a schist contact zone with eight different springs at 1250 m in altitude (Dursun et al., 2016). Several springs with large

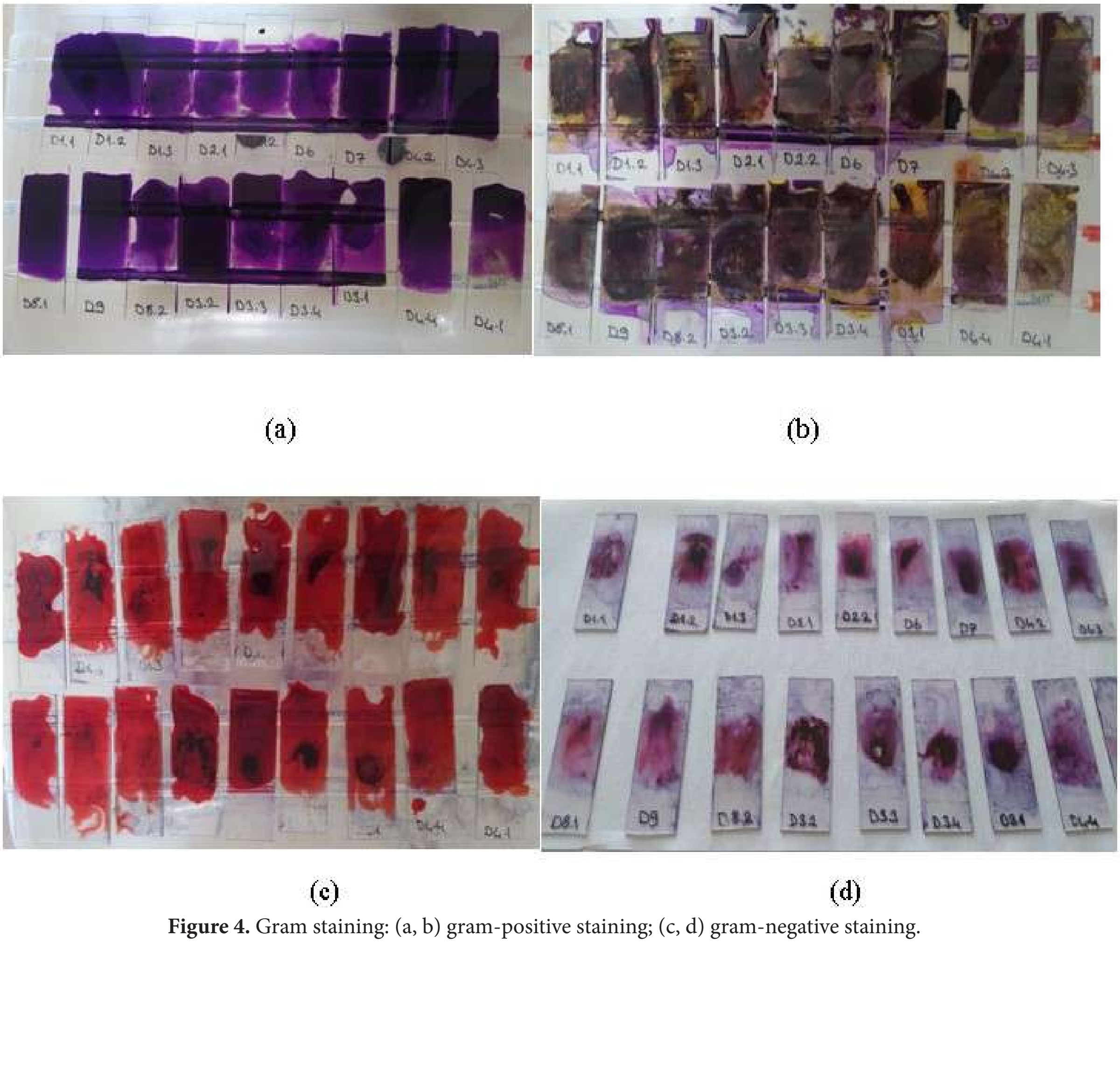

Figure 4. Gram staining: (a, b) gram-positive staining; (c, d) gram-negative staining.

Figure 5. Derme karstic springs (a, b) and karstic limestone soil cover (c).

and small flow potential are discharged from different parts of the limestone fracture zone including the fault, bedding, and joint system (Figures 5a and 5b). The Derme spring was significantly turbid after the earthquakes and the water turbidity then started to decrease over a long period of time. It became turbid again after each aftershock. Based on field observations, karstic limestone covers brown-colored alluvial and terra rosa soils in this region, as seen Figure 5c. The long-term average discharge flow rate of the Derme spring was 2.7 m^3/s; however, the spring's flow rate increased after postearthquake shocks. It can be suggested that the increase in spring flow rate occurred with the addition of new fracture systems or by the cleaning of sediments in the fractures during earthquake shaking. Although the turbidity gradually decreased after the earthquakes, aftershocks were observed to cause turbidity to increase again in this water source. Looking at changes in the physical properties of the water, the electrical conductivity of the Derme spring was measured as 278 **µ**S/cm in 2011 (Dursun et al., 2016), and the postearthquake measurement was 293 **µ**S/cm. In this case, a significant change in the amount of solid matter in the water was not observed, and it was understood that the turbidity did not affect the water characteristics due to the short water–rock interaction. Considering that the Derme spring meets the drinking water demands of about 750,000 people in Malatya, it is necessary to take measures to solve the turbidity problem.

Another karstic spring is located in the town of Bahçe in the province of Osmaniye, Türkiye. The Bahçe spring, which originates from Eocene-aged clayey limestone, did not flow for about 3 to 5 h after the earthquakes and then started to flow with a very intense turbidity based on local people's reports (Figure 6a). The turbidity continued for a long time and it was observed that the spring still flowed turbid in March, the month of the field survey. The formation of the region begins at the bottom with conglomerate and marl, where weak sequences of clayey and marl lithology play an important role in producing fine soil material that mixed with the groundwater after the seismic shocks (Figure 6b).

Another important karstic spring in the area is the Harbiye spring, which is discharged from the Cretaceous limestone in the Hatay region. The Harbiye spring is discharged from four different small-flow paths with a total flow rate of 0.8 m^3/s (Figure 6c). According to a previous study, the limestone comprises very dense karstic conduits including bedding, fracture, and fault zones (DSİ, 2019). The Harbiye spring was turbid after the earthquakes and returned to a normal level within a short period of time. Based on geological features, the limestone is laterally and vertically in contact with the red-colored ophiolitic series and it is thought that the red-colored ophiolitic materials were poured into the saturated zone from the limestone fracture and crack systems during the earthquake shocks. For this reason, the turbidity occurred in a short period of time and the color quickly returned to normal.

There are many karstic springs in the province of Gaziantep, such as the Akpınar, Kırkgöz, and Karpuzatan. In these karstic springs, significant turbidity did not occur after the earthquake shocks. The main reason for this is that soils that could cause turbidity problems are limited in Oligocene-aged limestones and Neogene-aged conglomerates (Şener et al., 2021). The soil cover, clay levels, and lithological features or bottom muds in the karst system are considered to be the most effective mechanisms for groundwater turbidity in the karst system. Therefore, more turbidity was observed in complex lithologies, while less turbidity was observed in more massive limestones. In the Elbistan plain, where another earthquake occurred, there are also allochthonous limestones. These limestones are highly productive and massive and have very limited soil cover. Groundwater discharged with a flow rate of over 50 L/s is carried out via the wells. Partial turbidity and odor

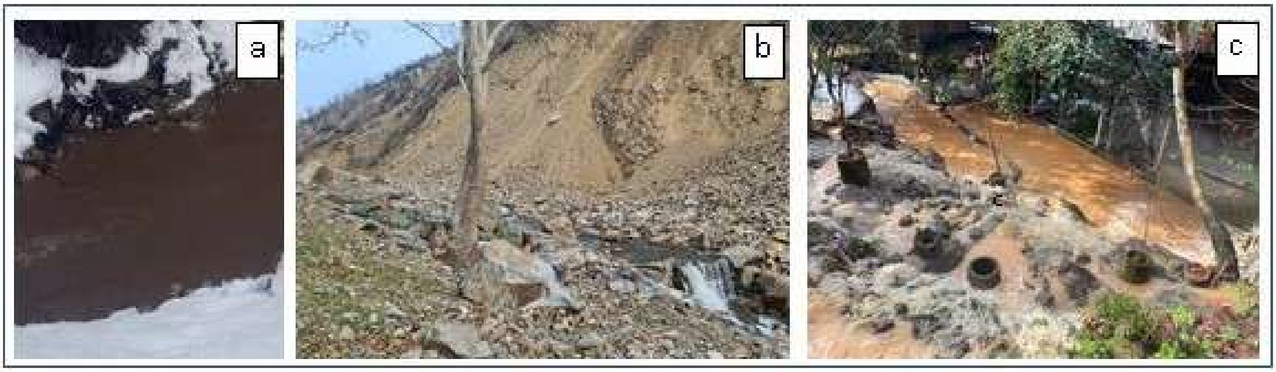

Figure 6. Osmaniye Bahçe spring (a), conglomerate-marl lithology (b), Hatay Harbiye spring (c).

were detected in the production wells, but these ended after a short time. The general mechanism of turbidity in the karst system due to earthquake shaking is presented in Figure 7.

Another important aquifer system in the earthquake zone consists of alluvial aquifers. Groundwater is discharged by wells in alluvial aquifers and used for drinking and irrigation purposes. The liquefaction problem caused by the earthquakes in the plain where the fault zone extends caused significant damage to structures and wells supplying groundwater from alluvial aquifers. Significant settlement problems due to liquefaction occurred in the coastal alluvial aquifer very close to the seashore and many settlement areas were found to be filled with seawater (Figure 8a). In the field study, it was also observed that some wells in the alluvial aquifer were deformed and/or collapsed due to soil liquefaction (Figure 8b). In addition, there are densely built-up industrial and residential areas on the alluvial aquifer. The lines supplying drinking water to the cities in these regions and the sewage systems were found to have suffered significant damage. In areas with liquefaction problems, such as İskenderun, the treatment facilities were damaged and remained inoperable due to structural damages. In this case, it is thought that there is a risk of groundwater contamination in the alluvial aquifer, and especially in the drinking water and sewage system, as seen in Figures 8c and 8d.

4.2. Physicochemical properties of waters after the earthquakes

Regarding the groundwater physicochemical characteristics, both springs and wells are discussed here. Physical parameters are shown in Table 2. The electrical conductivity (EC) of the sample from the spring in the mountainous area of Osmaniye-Bahçe was very high, revealing the presence of dissolvable salts in the area's geochemical structure, while oxygen saturation was very low. The EC value of this sample exceeded the Category A1 limit of 2500 µS/cm and fell into Category 3 (Official Gazette of the Republic of Türkiye, 2019). In other spring water samples, EC values exhibited Category A1 profiles. The pH and EC values of the spring waters from Osmaniye-Bahçe show that the origins of these waters are different, even though their distance from others is just a few kilometers. It was seen that spring waters from Hatay were of high quality based on the corresponding parameters, as were the spring waters from Malatya. The Horata 1 and Horata 2 samples showed identical characteristics; therefore, their source was understood to be the same (Figure 9).

The only groundwater (GW) sample exceeding the Category A1 limit for EC was obtained from the Hatay city center with a level of 13,420 µS/cm, while the pH value of this sample was the lowest among all samples (Figure 10). The other GW EC levels were below the limit of 2500 µS/cm for Category A1 waters. The oxygen saturation values of most GW samples were above 80%; however, the oxygen saturations of an unused well in the Gaziantep waste water treatment plant (WWTP) and another in the Hatay WWTP were measured as 60.5% and 76.8%, respectively. The pH values of groundwater well samples were in the range of Category A1 (Official Gazette of the Republic of Türkiye, 2019), except for a sample from the Hatay city center. Since the samples taken in Hatay were from a deformed alluvial aquifer, higher EC concentrations compared to samples from the other sites were detected due to liquification.

The EC and pH values of tap water samples were in the range of Category A1 waters. The oxygen saturation levels of these waters were above 80%, except for a sample collected from Gaziantep-Nurdağı, which was measured as 50% (Figure 11).

One of the intrusion water samples from Hatay-İskenderun was collected from sea water that had moved ashore; the electrical conductivity was measured as 52,500 µS/cm, reflecting a strong brackish water characteristic, while the sea water EC value was 58,000 µS/cm. This finding shows that this sample mainly comprised sea intrusion water slightly mixed with other less saline

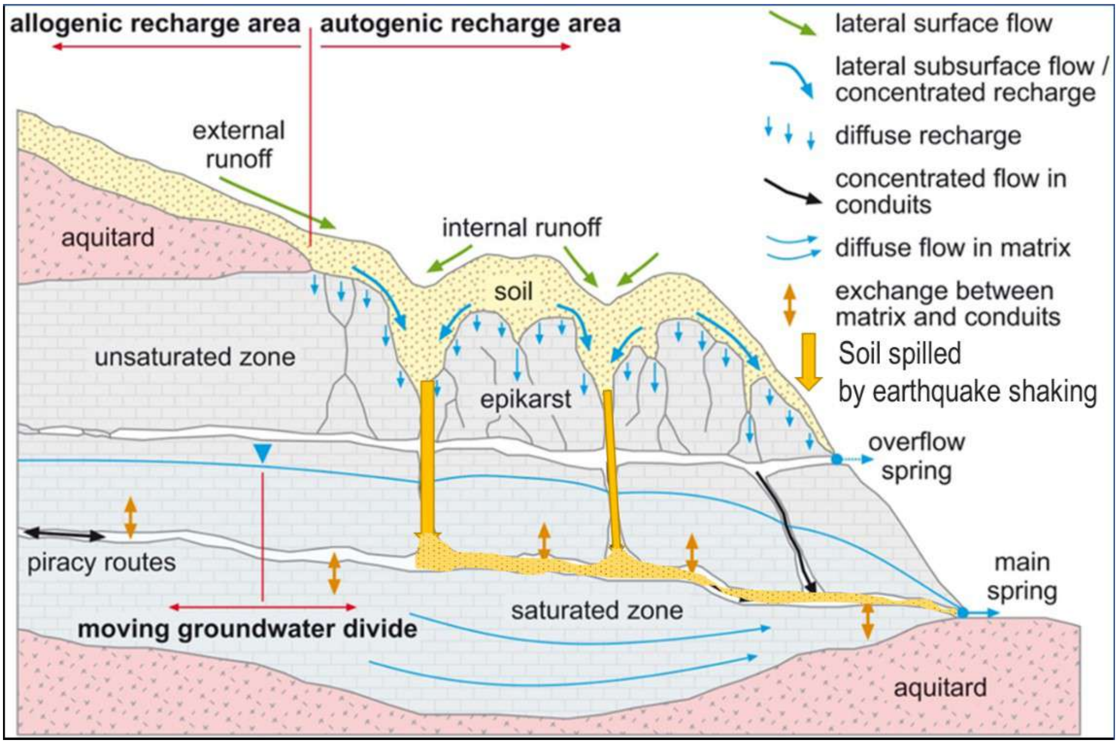

Figure 7. Conceptual model of turbidity mechanism in a karst system due to earthquake shaking (modified from Hartmann et al., 2014).

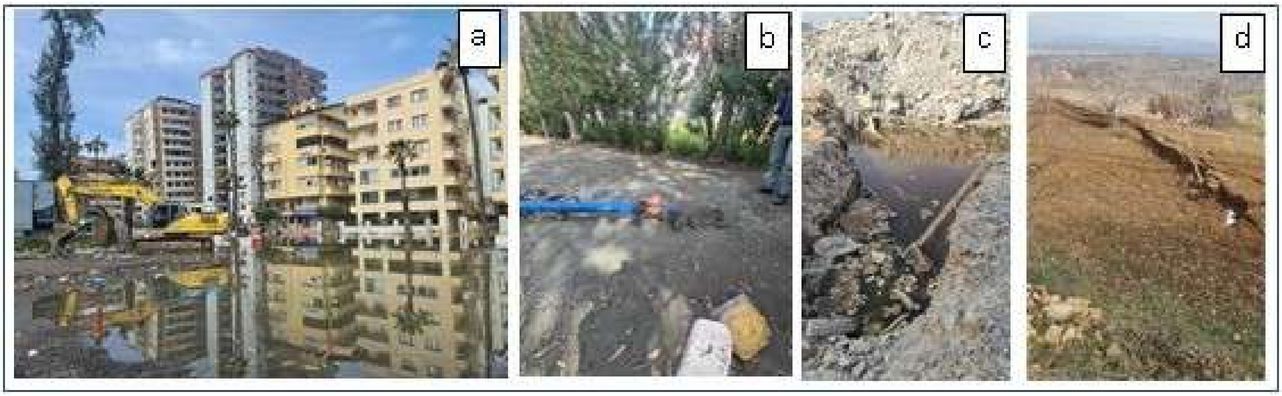

Figure 8. Some structural deformations of the alluvial aquifer.

water sources on the land. The oxygen saturation of the sample was 97%. Another sample from the bottom floor of a building showed lower oxygen saturation (53%) and a lower level of dissolved salts (15,250 µS/cm) (Figure 12).

4.3. Microbiological properties of waters

We analyzed aerobic colony counts measured in square centimeters for samples taken from various water sources. The findings are summarized in Table 2. The aerobic colony counts varied between 0.167 and 5.698 CFU/cm^2 in spring waters and the highest value was measured in Hatay's Harbiye spring. The aerobic colony counts in groundwater wells drilled in karst and alluvial aquifers in the region varied between 0.0185 and 7.16 CFU/cm^2. High colony count values were measured in the wells located

Table 2. In situ measurements and colony counts from cultivated water samples.

Sampling location	T (°C)	pH	Salinity	EC (µS/cm)	Dissolved oxygen (mg/L)	Dissolved oxygen (%)	Colony count (CFU/cm^2)
Water treatment plants							
Hatay-Karaçay WTP-Inlet	11.9	7.95	0.1	350	9.9	95.0	nd
Hatay-Karaçay WTP-Outlet	12.2	7.68	0.1	361	10.76	101.6	nd
Adana-Çatalan WTP-Inlet	19.8	8.04	0.1	412	8.89	94.4	nd
Adana-Çatalan WTP-Outlet	18.8	7.70	0.1	422	9.15	98.8	2.294
Kahramanmaraş-Ayvalı WTP-Inlet	14.4	7.48	0.1	368	8.39	89.1	nd
Kahramanmaraş-Ayvalı WTP-Outlet	14.1	7.83	0.1	369	10.01	103.7	0.204
Spring waters							
Osmaniye-surfaced spring water-city center	13.5	9.13	0.1	432	9.5	97.9	0.167
Osmaniye-surfaced spring water-mountainous area	28.1	7.93	7.9	13420	3.1	39.0	0.0185
Hatay-Harbiye Waterfall-surfaced spring water	17.4	7.94	0.1	464	9.52	100.9	5.698
Hatay-karst spring*	8.0	7.72	0.2	598	10.5	98.9	0.056
Malatya-Horata 1-surfaced spring water in channel	13.2	7.84	0.0	278	9.4	102.6	0.0185
Malatya-Horata 2-surfaced spring water in river bed	13.8	7.90	0.0	278	9.55	105.1	0.888
Malatya-Gündüzbey Kaptaj	12.1	7.91	0.0	293	9.51	101.0	0.185
GWWs							
Gaziantep-GWW next to Turgut Özal Viaduct*	8.0	8.13	0.30	687.00	11.24	100.3	0.0185
Gaziantep-karst GWW operated by municipality	19.5	6.71	0.20	512.00	7.72	87.1	0.444
Gaziantep-GWW-operated by municipality	20.9	6.60	0.10	429.00	7.43	88.2	3.293
Gaziantep-wastewater treatment plant GWW (unused)	20.7	6.55	0.20	660.00	5.50	60.5	0.148
Gaziantep-cooking oil industry GWW*	8.0	7.82	0.40	870.00	10.47	99.0	4.126
Hatay-GWW in oil station	16.2	8.12	0.20	582.00	9.76	101.2	0.056
Hatay-GWW in city center*	8.0	5.60	7.60	13520.00	10.01	91.1	3.256
Hatay-GWW in biological WWTP	20.5	8.12	1.3	2500	6.78	76.8	0.389
Adana-district GWW	20.4	7.14	0.20	659.00	9.02	99.6	0.093
Adana-GWW of a farm	20.6	7.05	0.70	1438.00	5.90	64.5	0.648
Gaziantep-GWW at water network start point	16.5	7.70	0.10	465.00	9.22	100.4	7.160
Gaziantep-GWW in central bus station	16.9	7.27	0.30	596.00	8.69	94.2	0.315
Kahramanmaraş-municipality construction site GWW	17.8	7.20	0.20	611.00	8.26	91.8	0.389
Kahramanmaraş-coal mining site-GWW in gyttja	13.3	7.51	0.20	591.00	7.68	82.9	0.907
Kahramanmaraş-coal mining site-GWW in karst	12.8	7.41	0.30	677.00	9.11	97.4	nd
Surface waters							
Gaziantep-Nizip Creek*	8.0	7.36	1	2060	10.9	99.3	3.478
Adana-Sanko Sanibey Dam tail water	23.5	7.72	0.2	510	9.8	95.1	nd
Tap water							
Hatay-Karaçay city center	15.7	7.71	0.1	359	10.18	104.1	3.996
Adana-Yüreğir WWTP	26.1	7.67	0.1	437	8.31	103.1	4.699
Gaziantep-small industrial site	21.4	7.88	0.1	300	4.00	50.0	11.674

Table 2. (Continued).

Kahramanmaraş-city center	14.2	7.28	0.1	365	9.83	102.8	0.278
Gaziantep-city center	21.4	7.64	0.3	693	6.6	81.0	0.093
Kahramanmaraş-city center	15.0	7.57	0.1	457	8.84	100.0	0.148
Malatya-Teknokent-container city	14.9	7.49	0.1	291	9.71	108.1	0.0185
Intrusion water							
Hatay-intrusion water from bottom floor of a building	19.8	7.82	8.8	15250	5.27	53.0	nd
Hatay-intrusion water from earth surface	20.6	7.83	33.7	52500	8.70	97.0	nd

*: Physicochemical parameters were measured in the laboratory.
nd: Not detected.

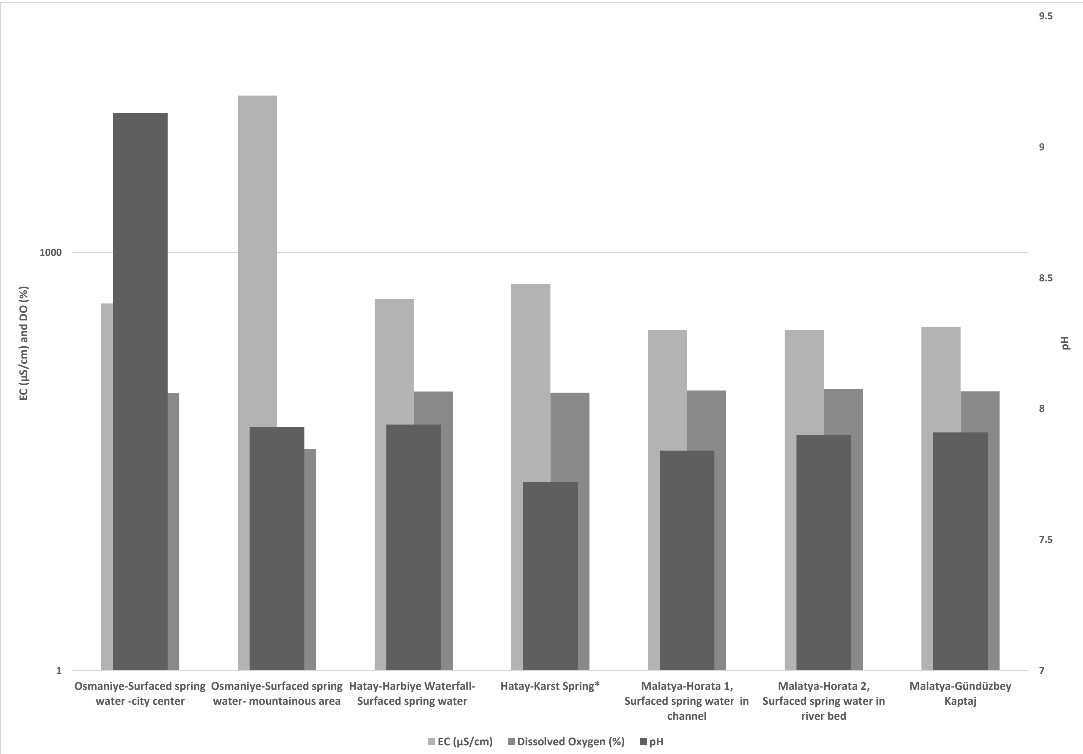

Figure 9. Electrical conductivity, dissolved oxygen, and pH values of samples from springs. *: Physicochemical parameters were measured in the laboratory.

in residential areas. Samples taken from tap water used as drinking water in the region were found to have values between 0.0185 and 11.674 CFU/cm^2. The highest colony count values were measured in districts of Gaziantep, Hatay, and Adana-Yüreğir. Aerobic colony counts were generally not detected in water treatment plants, except in Adana and Kahramanmaraş provinces. Since the EC levels of tap waters were in the normal range, it could be concluded that the detected microbial colonies were not directly related to leakages from sewage networks and other entrances into the water networks, such as soil particles due to the displacement of earth, should be considered.

Our results revealed that pollution levels were notably high in tap water, while well and spring water sources tended to have lower levels of contamination. However, it is important to note that even when the pollution levels in some well and spring water sources are lower compared to tap water, they still pose a risk to public health. It is also noteworthy that the clean water was polluted due to

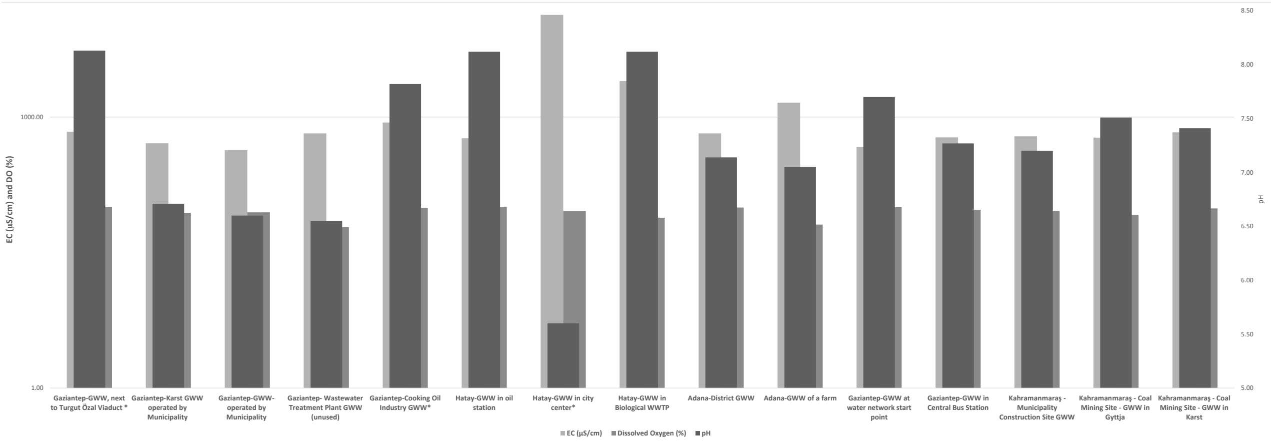

Figure 10. Electrical conductivity, dissolved oxygen, and pH values of samples from groundwater wells (GWWs). *: Physicochemical parameters were measured in the laboratory.

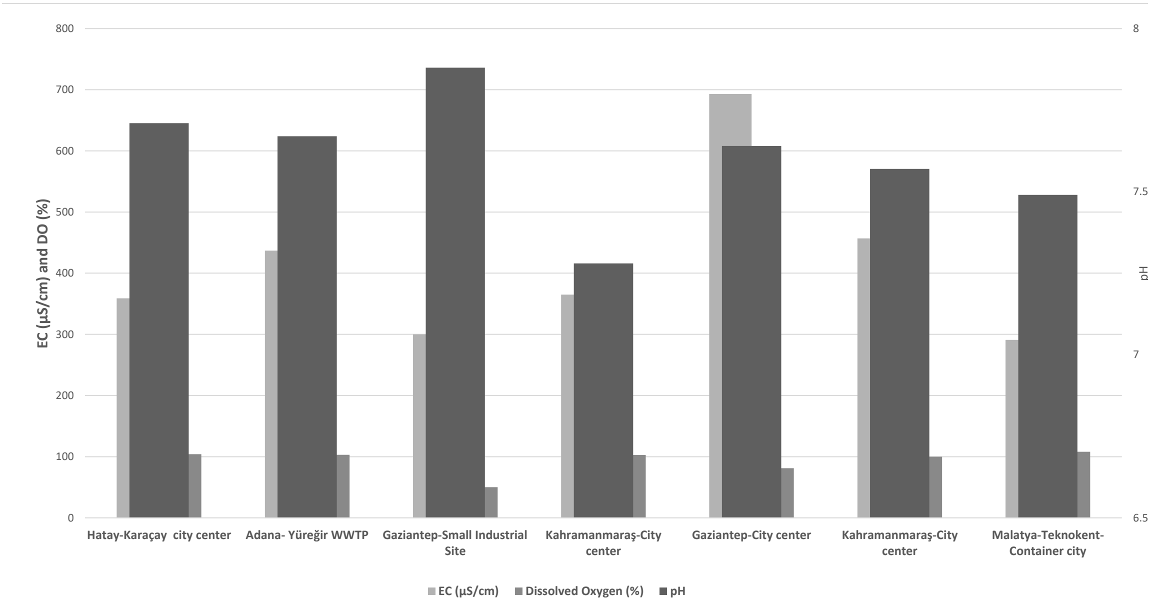

Figure 11. Electrical conductivity, dissolved oxygen, and pH values of samples from tap waters.

damage in the water distribution system in the section from the main water source to the tap water.

Our analysis indicates that the natural system of groundwater stabilizes relatively quickly after an earthquake, leading to a decrease in the associated risks. However, the risks associated with tap water continue to persist. This highlights the importance of monitoring and addressing the factors contributing to the contamination of tap water.

Furthermore, this study emphasizes that an increase in aerobic bacterial colony counts is an indicator of organic pollution. This finding suggests the presence of both bacterial and viral pathogens in the water sources, necessitating further research to fully understand the

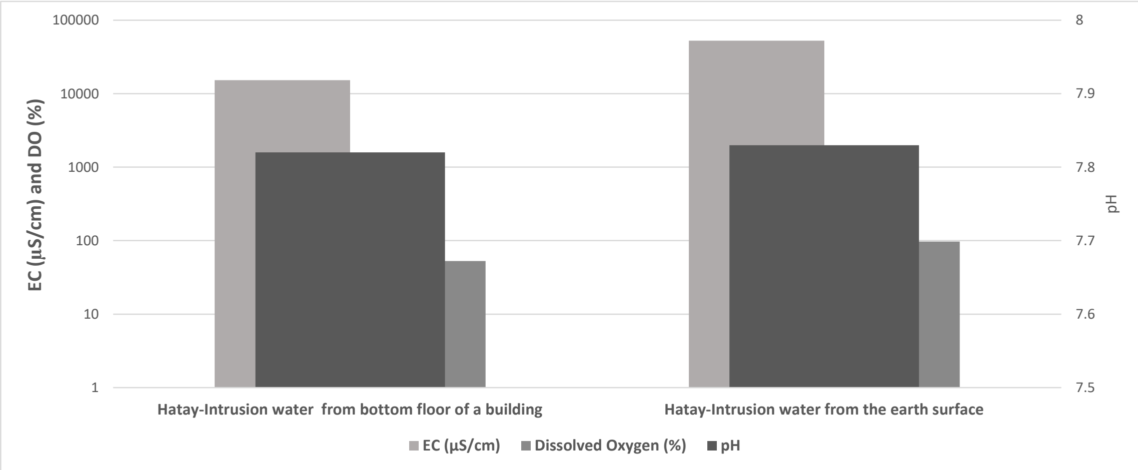

Figure 12. Electrical conductivity, dissolved oxygen, and pH values of samples from intrusion waters.

potential health implications. It is crucial to conduct additional studies to assess the presence and concentration of various pathogens in water samples, as this information is vital for designing appropriate water treatment and management strategies to ensure public health and safety.

It was seen that the deformation of the waterline system caused acute water shortage in the earthquake zone. In this context, ensuring the safety of water resources against natural disasters will reduce future problems.

5. Conclusions and suggestions

Various water samples collected from different water environments ranging from groundwater to tap water in the Kahramanmaraş earthquake region were investigated to evaluate the current state of the area's water supply systems. The findings of this study revealed that the turbidity level of groundwater in the karstic region is an important physical indicator of the impacts of the catastrophic Kahramanmaraş earthquakes on water resources. The karstic aquifer covered with terra rosa soil was proven to feed a number of high-discharge springs around the mountain, which are used as sources of drinking water in the earthquake region. Increased turbidity was frequently observed in groundwater resources from karstic aquifers in the earthquake zone and it was observed that lithological and soil cover factors played important roles in turbidity. In addition, in alluvial areas, structural damages caused by deformations due to liquefaction caused significant damage to wells supplying water.

This study also revealed that tap water samples were the most affected samples among those collected from the earthquake region due to the damage that occurred in network pipelines as a result of seismic waves. Very interesting findings were also obtained by co-evaluation of the data on colony counts and the physicochemical characteristics of the samples. The spring water from the mountainous area of Osmaniye-Bahçe, which had high EC (13,420 µS/cm) and low oxygen saturation (39%), was one of the samples with a lower colony count. This may be a result of the toxic impact of some dissolved heavy metals present in rock forms in the region. It was concluded that although there was no significant change in the water quality at the source, the probability of contamination was quite high due to deformations in the water networks of residential areas. Therefore, a comprehensive study is required to determine the major and minor elements of the waters of the region.

The following suggestions are presented in terms of protecting water resources and taking the necessary measures quickly in earthquake zones:

- Although there are short-term problems with groundwater resources right after an earthquake, they are the most reliable source of potable water.
- The groundwater resources in earthquake zones should be investigated in detail by means of their specific characteristics in order to be used as alternative water sources.
- Pipes that are resistant to deformation should be used in pipelines and networks to avoid damages from earthquakes.
- Portable water treatment systems should be installed and kept ready in specified postearthquake zones in residential areas in the short term.
- Alternative sewage systems must also be installed and kept ready in specified postearthquake zones in potential earthquake areas.
- Substitutional wells selected and designated as emergency drinking water sources should be drilled

in high-risk areas, connected to a mobile treatment system, and kept ready.
- Sand filtration units should be included in treatment systems to remove the turbidity of karstic springs.
- To minimize earthquake damages, all transmission pipes should be replaced with high-density polyethylene pipes supported with full soil and sand backfill in the canal, and the ground should be improved in areas with a risk of liquefaction.
- The sewage distribution system in the study area, which was heavily damaged after the earthquakes, should be replaced with an earthquake-resistant and regionally monitored network.
- A sanitation monitoring system should be established to check the quality of water at the source and at the network units frequently.

Acknowledgments
This study was funded by the Scientific and Technological Research Council of Türkiye (TÜBİTAK-MAM) under the 1002-C program on post-disaster projects support and also by the Scientific Research Projects Program of Dokuz Eylül University (Contract Number: FBG-2023-3144). The authors are thankful to officials of the Ministry of Environment, Urbanization, and Climate Change in the earthquake region and to the administrations of AFAD, MASKİ, GASKİ, and KASKİ for their assistance during the field studies.

References

Aksoy E (1994). Geological characteristics of Pertek (Tunceli) surroundings and Pertek Thrust Fault. Fırat Üniversitesi Fen ve Mühendislik Bilimleri Dergisi 6 (2): 1-8 (in Turkish with an abstract in English).

Allen CR (1969). Active Faulting in Northern Turkey: Contribution No. 1577. Pasadena, CA, USA: Division of Geological Sciences, California Institute of Technology.

Altınlı İE (1963). Explanatory Text of the Geological Map of Turkey of 1: 500 000 scale; Erzurum. Ankara, Türkiye: MTA.

Ambraseys NN (1989). Temporary seismic quiescence: SE Turkey. Geophysical Journal International 96 (2): 311-331. https://doi.org/10.1111/J.1365-246X.1989.TB04453.X

Amoruso A, Crescentini L, Petitta M, Rusi, Tallini M (2011). Impact of the 6 April 2009 L'Aquila earthquake on groundwater flow in the Gran Sasso carbonate aquifer, Central Italy. Hydrological Processes 25: 1754-1764. https://doi.org/10.1002/HYP.7933

Arpat E, Şaroğlu F (1972). The East Anatolian fault system; thoughts on its development. Bulletin of the Mineral Research and Exploration 78 (78): 33-39.

Beyarslan M, Bingöl AF (2018). Zircon U-Pb age and geochemical constraints on the origin and tectonic implications of late cretaceous intra-oceanic arc magmatics in the Southeast Anatolian Orogenic Belt (SE-Turkey). Journal of African Earth Sciences 147: 477-497. https://doi.org/10.1016/J.JAFREARSCI.2018.07.001

Cheong JY, Hamm SY, Kim SH, Lee SH, Woo NC et al. (2013). Analyzing groundwater change on a volcanic island caused by the impact of the M9 Sumatra earthquake. Geosciences Journal 2013: 17 (2): 183-195. https://doi.org/10.1007/S12303-013-0012-4

Chia Y, Chiu JJ, Chiang YH, Lee TP, Liu CW (2008). Spatial and temporal changes of groundwater level induced by thrust faulting. Pure and Applied Geophysics 165: 5-16. https://doi.org/10.1007/s00024-007-0293-5

Cox SC, Rutter HK, Sims A, Manga M, Weir JJ et al. (2012). Hydrological effects of the M_w 7.1 Darfield (Canterbury) earthquake, 4 September 2010. New Zealand Journal of Geology and Geophysics 55 (3): 231-247. https://doi.org/10.1080/00288306.2012.680474

Duman TY, Emre Ö (2013). The East Anatolian Fault: Geometry, segmentation and jog characteristics. Geological Society of London Special Publications 372 (1): 495-529. https://doi.org/10.1144/SP372.14

Dursun OF, Celiker M, Firat M (2016). Hydrological properties of the Derme karstic springs by using hydrogeochemical analyses and environmental isotope techniques. CLEAN – Soil, Air, Water 44 (2): 143-153. https://doi.org/10.1002/CLEN.201400035

DSİ (2019). Hatay-Harbiye Karst Su Kaynaklarının Hidrojeolojik Etüdü. Ankara, Türkiye: General Directorate of State Hydraulic Works (in Turkish).

Favere J, Barbosa RG, Sleutels T (2021). Safeguarding the microbial water quality from source to tap. NPJ Clean Water 4: 28. https://doi.org/10.1038/s41545-021-00118-1

Hosono T, Yamada C, Shibata T, Tawara Y, Wang CY et al. (2019). Coseismic groundwater drawdown along crustal ruptures during the 2016 Mw 7.0 Kumamoto earthquake. Water Resources Research 55: 5891-5903. https://doi.org/10.1029/2019WR024871

Ito Y, Malla SS, Bhattarai AP, Haramoto E, Shindo J et al. (2020). Waterborne diarrhoeal infection risk from multiple water sources and the impact of an earthquake. Journal of Water and Health 18 (4): 464-476. https://doi.org/10.2166/WH.2020.223

Karabacak V, Özkaymak Ç, Sözbilir H, Tatar O, Aktuğ B et al. (2023). The 2023 Pazarcık (Kahramanmaraş, Türkiye) earthquake (M_W: 7.7): implications for surface rupture dynamics along the East Anatolian Fault Zone. Journal of the Geological Society 180 (3): jgs2023-020. https://doi.org/10.1144/JGS2023-020

Karmakar S, Rathore AS, Kadri SM, Dutt S, Khare S et al. (2008). Post-earthquake outbreak of rotavirus gastroenteritis in Kashmir (India): an epidemiological analysis. Public Health 122 (10): 981-989. https://doi.org/10.1016/J.PUHE.2008.01.006

Ketin İ (1966). Anadolu'nun tektonik birlikleri. MTA Dergisi 66: 20-36 (in Turkish).

Kuraoka S, Rainer JH (1996). Damage to water distribution system caused by the 1995 Hyogo-ken Nanbu earthquake. Canadian Journal of Civil Engineering 23 (3): 665-677. https://doi.org/10.1139/L96-882

Lee HA, Woo NC (2012). Influence of the M9.0 Tohoku earthquake on groundwater in Korea. Geosciences Journal 16: 1-6. https://doi.org/10.1007/S12303-012-0010-Y

Maleki F, Hemati S, Pourashraf R (2020). Prevalence waterborne infections after earthquakes considered as serious threat to increasing victims in disaster-affected areas. Egyptian Journal of Veterinary Sciences 51 (1): 111-117. https://doi.org/10.21608/EJVS.2019.18629.1114

Mohr CH, Manga M, Wang CY, Kirchner JW, Bronstert A (2015). Shaking water out of soil. Geology 43 (3): 207-210. https://doi.org/10.1130/G36261.1

Nakagawa K, Shimada J, Yu ZQ, Ide K, Berndtsson R (2020). Effects of the Japanese 2016 Kumamoto earthquake on nitrate content in groundwater supply. Minerals 2021; 11 (1): 43. https://doi.org/10.3390/MIN11010043

Nakagawa K, Yu ZQ, Berndtsson R, Kagabu M (2019). Analysis of earthquake-induced groundwater level change using self-organizing maps. Environmental Earth Sciences 78: 455. https://doi.org/10.1007/s12665-019-8473-z

Official Gazette of the Republic of Türkiye (2019). İçme Suyu Temin Edilen Suların Kalitesi ve Arıtılması Hakkında Yönetmelik. Ankara, Türkiye: Directorate of Presidential Administrative Affairs. Available at https://www.resmigazete.gov.tr/eskiler/2019/07/20190706-8.htm (in Turkish).

Saroglu F, Emre O, Kuscu I (1992). The East Anatolian fault zone of Turkey. Annales Tectonicae 6: 99-125.

Sato T, Sakai R, Furuya K, Kodama T (2000). Coseismic spring flow changes associated with the 1995 Kobe earthquake. Geophysical Research Letters 27 (8): 1219-1222. https://doi.org/10.1029/1999GL011187

Scawthorn C, Johnson GS (2000). Preliminary report: Kocaeli (Izmit) earthquake of 17 August 1999. Engineering Structures 22 (7): 727-745. https://doi.org/10.1016/S0141-0296(99)00106-6

Schiff AJ (1995). Northridge Earthquake: Lifeline Performance and Post-Earthquake Response. Technical Council on Lifeline Earthquake Engineering Monograph No. 8. Reston, VA, USA: ASCE.

Şener Ş, Şener E, Er A (2021). Gaziantep ili yeraltısularının hidrojeokimyasal özellikleri Ve su kalitesi. Mühendislik Bilimleri ve Tasarım Dergisi 9 (4): 1253-1266 (in Turkish). https://doi.org/10.21923/JESD.927408

Şengör AMC, Görür N, Şaroğlu F (1985). Strike-slip faulting and related basin formation in zones of tectonic escape: Turkey as a case study. In: Biddle KT, Christie-Blick N (editors). Strike-Slip Deformation, Basin Formation, and Sedimentation. Tulsa, OK, USA: Society for Sedimentary Geology, pp. 211-226. https://doi.org/10.2110/PEC.85.37.0211

Singh VS (2008). Impact of the earthquake and tsunami of December 26, 2004, on the groundwater regime at Neill Island (south Andaman). Journal of Environmental Management 89 (1): 58-62. https://doi.org/10.1016/J.JENVMAN.2007.01.049

Skelton A, Andrén M, Kristmannsdóttir H, Stockmann G, Mörth CM et al. (2014). Changes in groundwater chemistry before two consecutive earthquakes in Iceland. Nature Geoscience 7: 752-756. https://doi.org/10.1038/ngeo2250

Tatar O, Piper JDA, Park RG, Gürsoy H (1995). Palaeomagnetic study of block rotations in the Niksar overlap region of the North Anatolian Fault Zone, central Turkey. Tectonophysics 244 (4): 251-266. https://doi.org/10.1016/0040-1951(94)00241-Z

TÜİK (2023). Adrese Dayalı Nüfus Kayıt Sistemi Sonuçları. Ankara, Türkiye: TÜİK (in Turkish)

Tulchinsky TH (2018). John Snow, cholera, the Broad Street Pump; Waterborne diseases then and now. In: Tulchinsky TH (editor). Case Studies in Public Health. Amsterdam, the Netherlands: Elsevier, pp. 77-99. https://doi.org/10.1016/B978-0-12-804571-8.00017-2

Wang CY, Manga M (2015). New streams and springs after the 2014 Mw6.0 South Napa Earthquake. Nature Communications 6: 7597. https://doi.org/10.1038/ncomms8597

WHO (2008). Guidelines for Drinking-Water Quality, 3rd Edition: Volume 1 - Recommendations Incorporating the First and Second Addenda. Geneva, Switzerland: World Health Organization. Available at https://www.who.int/publications/i/item/9789241547611

Zare MR, Wilkinson S, Potangaroa R (2010). Vulnerability of wastewater treatment plants and wastewater pumping stations to earthquakes. International Journal of Strategic Property Management 14 (4): 408-420. https://doi.org/10.3846/IJSPM.2010.30